

Effective two-mode model in Bose-Einstein condensates versus Gross-Pitaevskii simulations

Mauro Nigro^{1,2,a}, Pablo Capuzzi^{1,2,b}, Horacio M. Cataldo^{1,2,c}, and Dora M. Jezek^{1,2,d}

¹ Universidad de Buenos Aires, Facultad de Ciencias Exactas y Naturales, Departamento de Física, Pabellón 1, Ciudad Universitaria, 1428 Buenos Aires, Argentina

² Instituto de Física de Buenos Aires, CONICET-UBA, Pabellón 1, Ciudad Universitaria, 1428 Buenos Aires, Argentina

February 27, 2018

Abstract. We study the dynamics of three-dimensional Bose-Einstein condensates confined by double-well potentials using a two-mode model with an effective on-site interaction energy parameter. The effective on-site interaction energy parameter is evaluated for different numbers of particles ranging from a low experimental value to larger ones approaching the Thomas-Fermi limit, yielding important corrections to the dynamics. We analyze the time periods as functions of the initial imbalance and find a closed integral form that includes all interaction-driven parameters. A simple analytical formula for the self-trapping period is introduced and shown to accurately reproduce the exact values provided by the two-mode model. Systematic numerical simulations of the problem in 3D demonstrate the excellent agreement of the two-mode model for experimental parameters.

Key words. Bose-Einstein condensate – two-mode model – Josephson oscillations – self-trapping

PACS. XX.XX.XX No PACS code given

1 Introduction

The TM model applied to double-well atomic Bose-Einstein condensates has been extensively studied in the recent years [1–12]. Such a model assumes that the condensate order parameter can be described as a superposition of wave functions localized in each well with time dependent coefficients [1,2]. The localized wave functions are straightforwardly obtained in terms of the stationary symmetric and antisymmetric states, which in turn determine the parameters involved in the TM equations of motion [1–4]. The corresponding dynamics exhibits Josephson and self-trapping regimes [1,2] which have been experimentally observed by Albiez *et al.* [5].

The self-trapping (ST) phenomenon, which is also present in extended optical lattices [13–18], is a non linear effect where the difference of populations between neighbouring sites does not change sign during the whole time evolution. There is nowadays an active research on the ST effect, which involves different types of systems, including mixtures of atomic species [6, 19]. Research on condensates trapped in ring-shaped optical lattices is also a promising area given that successful efforts has been

done in their experimental realization [20]. The dynamics on systems with three [21] and four wells [22] has been initially investigated through multimode models that utilized *ad-hoc* values for the hopping and on-site energy parameters. Whereas in [23], such parameters have been extracted for a ring-shaped optical lattice with an arbitrary number of wells, by constructing two-dimensional localized Wannier-like (WL) functions in terms of stationary Gross-Pitaevskii (GP) states.

In recent works it has been shown that a correction in the TM model that involves the interaction energy should be taken into account in order to properly describe the exact dynamics [23, 24]. In particular in [24] an effective two-mode (ETM) model has been developed with an interaction parameter which has been analytically obtained in the Thomas-Fermi (TF) limit, that completely heals this disagreement. In the present work, we will extend these studies for lower numbers of particles by numerically calculating the effective parameter that enters in the model. Here we will analyze the double-well system with the experimental conditions of [5], where the number of particles is 1150, and increase such a number to show that the correction to the on-site interaction energy parameter goes to the one predicted in the TF regime [24]. The main goal of this work is to assess the accuracy of the ETM model by calculating the time periods as functions of the initial imbalance and analyze the role of the different parameters. To this end, we shall confront the values of the orbits peri-

^a e-mail: nigro@df.uba.ar

^b e-mail: capuzzi@df.uba.ar

^c e-mail: cataldo@df.uba.ar

^d e-mail: djezek@df.uba.ar

ods predicted by this model to those obtained by numerically solving the three-dimensional Gross-Pitaevskii equations. In particular, within the effective two-mode model framework we derive closed expressions for the periods valid for any imbalance value. We then develop a simple analytical approximation to the ST period and improve the calculation of the Josephson period for small imbalances by taking into account the parameter that involves the density overlap between the localized states in neighbouring sites [3]. This correction will be of importance for the experimental configuration of the Heidelberg group [5]. We will show that the critical imbalance for the transition between the Josephson and ST regimes predicted by our model is in good agreement with the experimental finding in Ref. [25] for the first time.

This paper is organized as follows. In Sect. 2 we describe the double-well system and find the effective on-site interaction energy parameter for several particle numbers. Such a parameter is obtained from a linear approximation of the on-site interaction energy as a function of the imbalance. We will show that the corresponding second order term in the approximation turns out to be much smaller and gives rise to a third order correction in the equations of motion which can be safely disregarded. In Sect. 3 we derive a closed integral form for the period of the orbits with an arbitrary initial imbalance and obtain explicit analytical approximations within the ST and Josephson regimes, while the numerical results and comparisons with the GP calculations are included in Sect. 4. To conclude, a summary of our work is presented in Sect. 5 including a perspective of the application of these methods to multiple-well systems in configurations with high symmetries. Finally, the definition of the parameters employed in the equations of motion are gathered in the Appendix.

2 Two-mode model

We consider a Bose-Einstein condensate of Rubidium atoms confined by the external potential V_{trap} used in the experiment of the Heidelberg group [5],

$$V_{\text{trap}}(\mathbf{r}) = \frac{1}{2} m (\omega_x^2 x^2 + \omega_y^2 y^2 + \omega_z^2 z^2) + V_0 \cos^2(\pi x/q_0) \quad (1)$$

where m is the atom mass, $\omega_x = 2\pi \times 66$ Hz, $\omega_y = 2\pi \times 78$ Hz, and $\omega_z = 2\pi \times 90$ Hz. The lattice parameters are given by $V_0 = 2\pi \times 412 \hbar$ Hz and $q_0 = 5.2 \mu\text{m}$. The number of particles used in the experiment is $N = 1150$, but we will also consider particle numbers up to $N = 10^5$.

2.1 Inclusion of effective on-site interaction energy effects

In previous works [23, 24] we have shown that the linear dependence on the imbalance of the interaction energy integrated in each well gives rise to a lower effective on-site interaction parameter. Here we will evaluate such a

parameter by using a combination of the procedures described in [23, 24] and also by expanding to a higher order approximation on the imbalance.

In doing so, we first rewrite the TM equations of motion by assuming that the on-site interaction energy U can be different in the left (U_L) and right (U_R) wells. As described in [24], U_R and U_L arise from introducing in the mean-field interaction term of the GP equation a more realistic density distribution that depends on the imbalance. Then the GP equation projected into two localized modes at the left and right wells yields [3]

$$\hbar \frac{dZ}{dt} = -2K\sqrt{1-Z^2} \sin \varphi + I(1-Z^2) \sin 2\varphi \quad (2)$$

$$\hbar \frac{d\varphi}{dt} = U_R(Z)N_R - U_L(Z)N_L + 2K \left[\frac{Z}{\sqrt{1-Z^2}} \right] \cos \varphi - IZ(2 + \cos 2\varphi). \quad (3)$$

The dynamical variables are the standard imbalance $Z = (N_R - N_L)/N$ and phase difference $\varphi = \varphi_L - \varphi_R$, where N_R and N_L are the number of particles in the right and left wells, respectively. As derived in [24] we have

$$U_k(\Delta N) = g \int d^3\mathbf{r} \rho_N^k(\mathbf{r}) \rho_{N+\Delta N}^k(\mathbf{r}), \quad (4)$$

where $k = R, L$, and ρ_N^k , and $\rho_{N+\Delta N}^k$ are the localized densities in the k -site for systems with total number of particles N and $N + \Delta N$, respectively. The remaining parameters J , and the interaction-driven F and I are defined as usual [1–3] in terms of the localized wave functions (see the Appendix), being $K = J + F$.

Aiming at reproducing the experimental conditions of [5], where the number of particles $N = 1150$ is not large enough to be in the Thomas-Fermi regime, and thus the dependence on the imbalance of the on-site interaction energy U_R and U_L cannot be analytically calculated, we should evaluate Eq. (4). To simplify the numerical calculation given that the wells are equal, instead of using the localized densities in Eq. (4), we can use the alternative method proposed in [23] where only GP ground-state densities are involved. In that work it has been shown that $U_k(\Delta N_k)$ with $\Delta N_k = N_k - N/2$ can be evaluated as

$$\frac{U_k(\Delta N_k)}{U} = \frac{\int d^3\mathbf{r} \rho_N(\mathbf{r}) \rho_{N+\Delta N}(\mathbf{r})}{\int d^3\mathbf{r} \rho_N^2(\mathbf{r})}, \quad (5)$$

where ρ_N and $\rho_{N+\Delta N}$ are the GP ground-state densities for systems with N and $N + \Delta N$ total number of particles, respectively, being $\Delta N = 2\Delta N_k$. The numerical result of U_k/U as a function of $\Delta N/N$ has been depicted in Fig. 1, where it can be seen that it exhibits an almost linear behaviour. A second order approximation of U_k

$$\frac{U_k(\Delta N_k)}{U} \simeq 1 - \alpha \frac{2\Delta N_k}{N} + \beta \left(\frac{2\Delta N_k}{N} \right)^2 \quad (6)$$

can be obtained by using a polynomial fit of the function with parameters α and β . These parameters are listed in

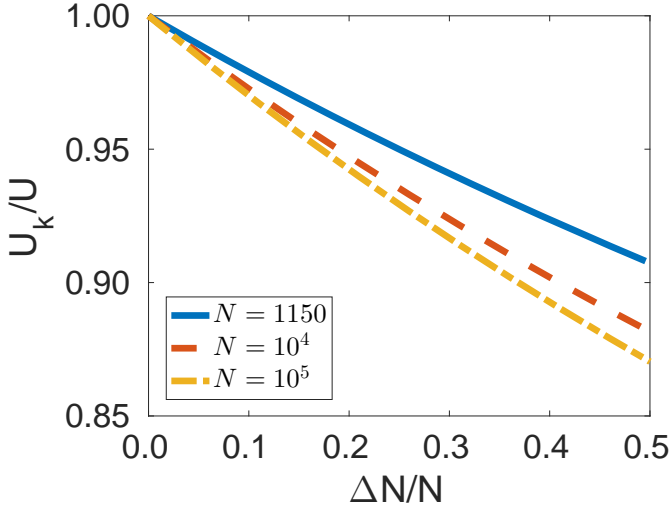


Fig. 1. (color online) On-site interaction energy ratio U_k/U as a function of $\Delta N/N$, for $N = 1150$, $N = 10^4$, and $N = 10^5$.

Table 1. Coefficients α and β of the quadratic fit of U_k/U as a function of $\Delta N/N$ and γ for several values of the system parameters. In the 6th column the factor f_{3D} that reduces the interaction energy parameter is also given.

N	q_0 (μm)	V_0 ($2\pi\hbar\text{Hz}$)	α	β	$f_{3D} = 1 - \alpha$	γ
1150	5.2	412	0.21	0.06	0.79	0.064
10^4	5.2	858	0.28	0.08	0.72	0.010
10^5	8.0	1980	0.30	0.08 ^a	0.70 ^b	0.005

^a The Thomas-Fermi limit is $77/1000$.

^b The Thomas-Fermi limit is $7/10$.

Table 1 for different numbers of particles and trapping parameters. It is worthwhile mentioning that for the largest number of particles considered in this work, we have taken a larger q_0 value than that of the Heidelberg experiment and modified the depth of the wells since the size of the condensate increases with the number of particles.

Introducing the expansions of U_R and U_L in the equation of motion (3) for the phase difference, we obtain the on-site interaction-driven correction,

$$\frac{U_R(\Delta N_R)}{U} N_R - \frac{U_L(\Delta N_L)}{U} N_L = [(1 - \alpha)Z + \beta Z^3] N, \quad (7)$$

which yields

$$\hbar \frac{d\varphi}{dt} = [(1 - \alpha)Z + \beta Z^3] UN + 2K \left[\frac{Z}{\sqrt{1 - Z^2}} \right] \cos \varphi - IZ(2 + \cos 2\varphi). \quad (8)$$

We note that for all number of particles of Table 1 we have $\beta Z^3 \ll (1 - \alpha)Z$, and hence one can safely disregard the term of third order in Z in Eq. (8) in all cases. Then, we conclude that the effective TM model can be simply obtained by replacing the on-site interaction energy parameter U by $U_{\text{eff}} = (1 - \alpha)U = f_{3D}U$. For the largest number of particles considered here, we have $f_{3D} = 7/10$ in accordance with the analytic result obtained in the

Thomas-Fermi approximation [24], whereas for the lowest value $N = 1150$, we obtain $f_{3D} = 0.79$. Such a value does not seem to depend on the ratio of the trap frequencies, since in [26] the harmonic trap frequencies are equal in the three directions and the same value of f_{3D} was also obtained.

2.2 Two-mode model using the effective interaction parameter

We now focus on the experimentally relevant case of $N = 1150$, where we have obtained the following TM model [3] parameters: $U = 2.47 \times 10^{-3} \hbar\omega_x$, $J = 1.89 \times 10^{-2} \hbar\omega_x$, $F = 2.51 \times 10^{-2} \hbar\omega_x$, and $I = 5.62 \times 10^{-3} \hbar\omega_x$. Using the results of the previous section, we obtain $U_{\text{eff}} = f_{3D}U = 1.95 \times 10^{-3} \hbar\omega_x$, with $f_{3D} = 1 - \alpha = 0.79$.

In terms of the conjugate coordinates, imbalance Z and phase difference φ , one can define the following ETM model Hamiltonian [24]:

$$H_{\text{ETM}}(Z, \varphi) = \frac{1}{2} \Lambda_{\text{eff}} Z^2 - \sqrt{1 - Z^2} \cos \varphi + \frac{\gamma}{2} (1 - Z^2) (2 + \cos 2\varphi), \quad (9)$$

with $\Lambda_{\text{eff}} = U_{\text{eff}}N/(2K)$ and $\gamma = I/(2K)$.

The corresponding equations of motion are given in Hamiltonian form by

$$\dot{Z} = -\frac{\partial}{\partial \varphi} H_{\text{ETM}}, \quad \text{and} \quad \dot{\varphi} = \frac{\partial}{\partial Z} H_{\text{ETM}} \quad (10)$$

which yield

$$\frac{dZ}{dt} = -\sqrt{1 - Z^2} \sin \varphi + \gamma(1 - Z^2) \sin 2\varphi \quad (11)$$

$$\frac{d\varphi}{dt} = \Lambda_{\text{eff}} Z + \left[\frac{Z}{\sqrt{1 - Z^2}} \right] \cos \varphi - \gamma Z(2 + \cos 2\varphi), \quad (12)$$

where the time t is given in units of $\hbar/2K$.

The separatrix between Josephson and ST orbits on the phase portrait (Z, φ) has a critical imbalance Z_c determined by the condition $H(Z_c, 0) = H(0, \pi)$, which yields

$$Z_c^{\text{ETM}} = 2 \frac{\sqrt{\Lambda_{\text{eff}} - 3\gamma - 1}}{\Lambda_{\text{eff}} - 3\gamma}. \quad (13)$$

Using $\Lambda_{\text{eff}} = 25.5$ we obtain a critical imbalance $Z_c^{\text{ETM}} = 0.389$ which is much closer to that numerically found, $Z_c^{\text{GP}} = 0.39$, than the value $Z_c^{\text{TM}} = 0.347$ obtained with the bare $\Lambda = 32.27$ from the TM-model version improved by Ananikian *et al.* [3]. We also note that the effect of γ is negligible in the Z_c calculation. The numerical value of Z_c^{GP} was obtained by analyzing the time evolutions of the GP equation with different initial conditions as done in [6]. In contrast to previous approximations, the value of Z_c^{ETM} compares very well with the experimental finding of the Heidelberg group as indicated in [25].

We can estimate the relative deviation between the ETM and TM models as

$$\frac{\Delta Z_c}{Z_c^{\text{TM}}} \simeq \frac{1}{\sqrt{f_{3D}}} - 1, \quad (14)$$

which goes from 0.13 for $N = 1150$ to 0.2 for the largest N considered.

3 Two-mode model periods

3.1 Exact determination

The time periods of orbits in both the TM and ETM models can be obtained for any initial imbalance Z_i and phase difference φ_i . For a classical Hamiltonian system such as that described by Eq. (9) we can obtain the period τ from the line integral over a given trajectory, $\tau = -\oint 1/(\partial H/\partial \varphi) dZ$ [27]. Following this approach, an expression which does not include the parameter γ was previously obtained in [27, 28] for the TM model. Here we extend that result and show that an expression incorporating γ can also be achieved, demonstrating that this correction may be important in the Josephson regime.

The period τ of a given trajectory can be calculated from the integral $\tau = \oint (1/\dot{Z}) dZ$ where \dot{Z} is given by (11). The relation between Z and φ is obtained for a given energy E by setting $H(Z, \varphi) = E$, yielding a quadratic equation for $\cos \varphi$ with the solution $\cos \varphi = \frac{1}{2\gamma\sqrt{1-Z^2}}(1 - \sqrt{Y})$, where $Y = 1 - 2\gamma[(A - \gamma)Z^2 - 2E + \gamma]$. Taking this into account the time period is given by

$$\tau(Z_i, \varphi_i) = 2 \int_{Z_m}^{Z_M} dZ \frac{1}{\sqrt{Y}} \frac{1}{\sqrt{1 - Z^2 - \frac{1}{4\gamma^2}(1 - \sqrt{Y})^2}} \quad (15)$$

where Z_m (Z_M) is the minimum (maximum) imbalance reached by the system. The values of Z_m and Z_M are obtained from the phase diagram that emerges by setting $H = E$, and have different expressions depending on the regime. In the Josephson regime ($Z_M < Z_c$) the conditions are $H(Z_i, \varphi_i) = H(Z_M, 0) = H(Z_m, 0)$ with $Z_M > 0$, $Z_m = -Z_M$, which give

$$Z_M^m = \mp \sqrt{\frac{2}{A^2} [AB - 1 + \sqrt{C}]}, \quad (16)$$

where $A = \Lambda - 3\gamma$, $B = E - 3\gamma/2$ and $C = (AB - 1)^2 - A^2(B^2 - 1)$. On the other hand, in the ST regime, taking into account that the phase diagram is symmetric under the inversion of Z_i we restrict the domain of Z_i to $Z_i > 0$. In this case the conditions read $H(Z_i, \varphi_i) = H(Z_M, 0) = H(Z_m, \pi)$ valid for $Z_M > Z_c$, which yield

$$Z_M^m = \sqrt{\frac{2}{A^2} [AB - 1 \mp \sqrt{C}]}. \quad (17)$$

This formulation can also be used for the ETM model by replacing Λ by Λ_{eff} . It is worthwhile mentioning that the

expression (15) for $\gamma = 0$ can be written in terms of the complete Elliptic integral of the first kind $\mathcal{K}(k)$, as shown previously in [2] by directly integrating the equations of motion for $Z(t)$ and $\varphi(t)$.

3.2 Approximate expressions

Even though the above formalism provides a closed integral form for the time periods amenable to a numerical calculation, both in the Josephson and ST regimes, it is also useful to derive analytical expressions in specific limits. In the case of small oscillations, by retaining only quadratic terms in the Hamiltonian, Eq. (15) can be straightforwardly integrated and we recover the expressions given by the standard formula in [1, 6] with the inclusion of γ [3]. Replacing U by U_{eff} , one thus obtains the ETM model period,

$$T_{so}^{\text{ETM}} = \frac{\pi \hbar}{K \sqrt{(\Lambda_{\text{eff}} + 1 - 3\gamma)(1 - 2\gamma)}}, \quad (18)$$

which yields $T_{so}^{\text{ETM}} = 14.91 \omega_x^{-1}$ in contrast to $T_{so}^{\text{TM}} = 13.29 \omega_x^{-1}$ obtained using the bare Λ value. We remark that an important correction is also provided by the parameter γ . This correction diminishes for increasing Z_i , and it does not affect sizeably either the critical imbalance Z_c , or the time periods in the ST regime.

In the ST regime one can also derive a limiting approximation for the time period valid for large Λ . In this case, we can neglect γ and take the first-order approximation of the function $\mathcal{K}(k)$ around $k = 0$. This yields the analytical expression for the time period τ_0

$$\tau_0 = \frac{\hbar}{2K} \frac{2\pi}{\Lambda Z_i}. \quad (19)$$

A higher-order approximation of $\mathcal{K}(k)$ could also be employed to increase the accuracy of τ_0 , but since one should retain an important number of terms to achieve a noticeable improvement, this procedure become quite cumbersome thus relegating the simplicity of Eq. (19).

However, a simple analytical formula that improves τ_0 can be developed in the ST regime by performing some approximations directly in the equations of motion. We will keep assuming a large interaction parameter Λ and neglect the parameter γ , as it does not contribute to any significant change in the predictions of this regime. Considering the imbalance performs oscillations around a positive mean value and using $\Lambda \gg 1$, (12) can be approximated by,

$$\frac{d\varphi}{dt} = \Lambda Z + \left[\frac{Z}{\sqrt{1 - Z^2}} \right] \cos \varphi \simeq \Lambda Z \simeq \Lambda Z_0, \quad (20)$$

where $Z_0 = \overline{Z(t)}$ denotes the mean value of the time dependent imbalance, and we have used that the second term of Eq. (20) averages approximately to zero. Then, assuming $\varphi(0) = 0$ we obtain,

$$\varphi(t) = \Lambda Z_0 t, \quad (21)$$

which replaced in Eq. (11) with the further assumption that $\sqrt{1 - Z^2} \simeq \sqrt{1 - Z_0^2}$ yields,

$$\frac{dZ}{dt} = -\sqrt{1 - Z_0^2} \sin(\Lambda Z_0 t). \quad (22)$$

Integrating the last expression with respect to time and considering the initial value $Z(0) = Z_i$, we finally obtain for small Z_0^2

$$Z(t) = \left(1 - \frac{Z_0^2}{2}\right) \frac{\cos(\Lambda Z_0 t)}{\Lambda Z_0} - \left(1 - \frac{Z_0^2}{2}\right) \frac{1}{\Lambda Z_0} + Z_i. \quad (23)$$

Furthermore, to be consistent with Z_0 being the mean value of $Z(t)$, we impose

$$Z_0 = -\left(1 - \frac{Z_0^2}{2}\right) \frac{1}{\Lambda Z_0} + Z_i, \quad (24)$$

which yields a quadratic equation for Z_0 with the following solution for $\Lambda \gg 1$,

$$Z_0 = \frac{Z_i}{2} \left[1 \pm \sqrt{1 - \frac{4}{\Lambda Z_i^2}} \right]. \quad (25)$$

Given that we are assuming a ST regime, which implies that $Z(t)$ from Eq. (23) should not change sign during the evolution, we discard the minus sign in front of the square root in Eq. (25). Therefore, using Eq. (25) we can estimate the ST period $T_{st} = 2\pi/(\Lambda Z_0)$ as,

$$T_{st} = \frac{Z_i \pi \hbar}{2K} \left(1 - \sqrt{1 - \frac{4}{\Lambda Z_i^2}} \right), \quad (26)$$

which will be expressed in units of ω_x^{-1} . The above equation can also be used by replacing Λ by Λ_{eff} to better take into account the effective interaction effects. For example, for an initial imbalance $Z_i = 0.45$ it yields $T_{st}^{\text{ETM}} = 8.42 \omega_x^{-1}$ and $T_{st}^{\text{TM}} = 6.05 \omega_x^{-1}$ in comparison with that obtained with the GP simulation, $T_{st}^{\text{GP}} = 8.54 \omega_x^{-1}$.

4 Numerical results

Aiming at testing the validity of the model equations, we have numerically solved the GP equation using a second order in time, split-step spatial Fourier operator [29, 30] with up to $512 \times 512 \times 256$ grid points and time steps down to $\Delta t = 5 \times 10^{-5} \omega_x^{-1}$. In Figs. 2 and 3 we show the GP time evolutions for initial imbalances in the Josephson and ST regimes, respectively, as compared to those given by TM models using the bare Λ and the effective Λ_{eff} values. It becomes clear that the effective approach reproduces the GP results much better than the bare TM model in both regimes. We also notice that the small-oscillation period (18) calculated from the effective interaction parameter is a much better estimate and the same holds for the period estimates given by Eq. (26) in the ST regime.

In Fig. 4 we compare the time periods as a function of the imbalance using the TM and ETM models together

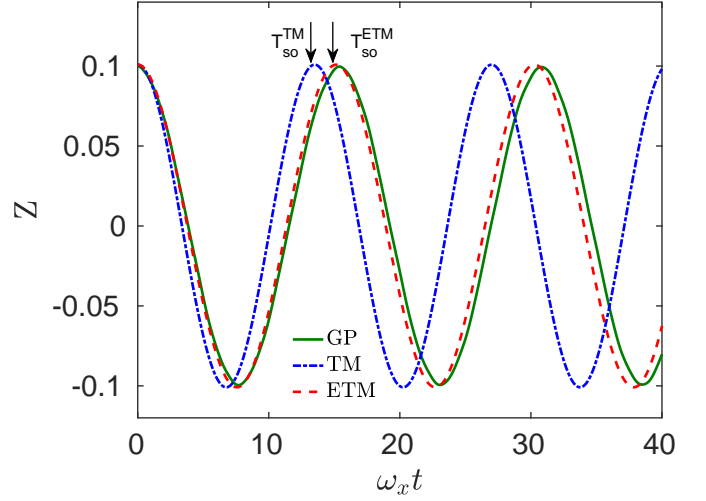


Fig. 2. (color online) Time evolution of an initial imbalance in the Josephson regime using the GP equation, the TM and ETM models for the initial condition $Z_i = 0.1$ and $\varphi_i = 0$. The vertical arrows indicate the small-oscillation period estimates for both models, Eq. (18).

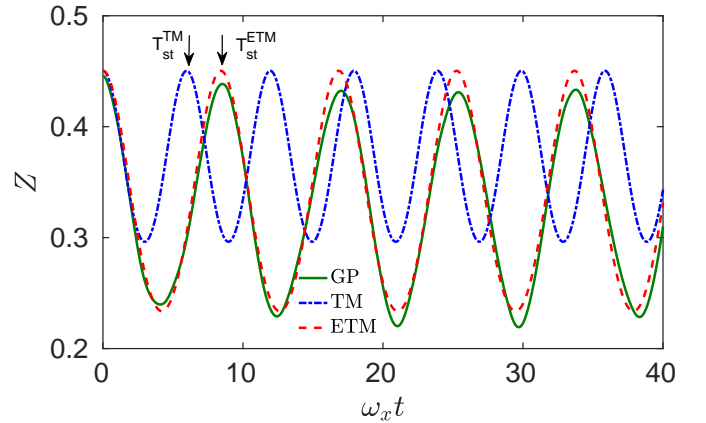


Fig. 3. (color online) Time evolution of an initial imbalance in the ST regime using the GP equation, the TM and ETM models for the initial condition $Z_i = 0.45$ and $\varphi_i = 0$. The vertical arrows indicate the ST period estimates arising from Eq. (26) for both models.

with several periods obtained from GP simulations. We also plot with empty circles $T_{st}(Z_i)$ from Eq. (26) and with horizontal lines T_{so} given by Eq. (18), both for the TM and ETM models. We notice that the predictions for both the ST and the small-oscillation periods are highly accurate within both two-mode models, and that the ETM results agree well with the full GP calculation. We have also included in Fig. 4 calculations neglecting γ (depicted in thinner lines), so as to emphasize that for the experimentally relevant case of $N = 1150$ the inclusion of the parameter γ also yields a sizable correction to the Josephson periods. On the other hand, for smaller overlaps between the densities of the localized states, the factor γ is substantially reduced (cf. Table 1) and thus it does not play any significant role in determining these periods.

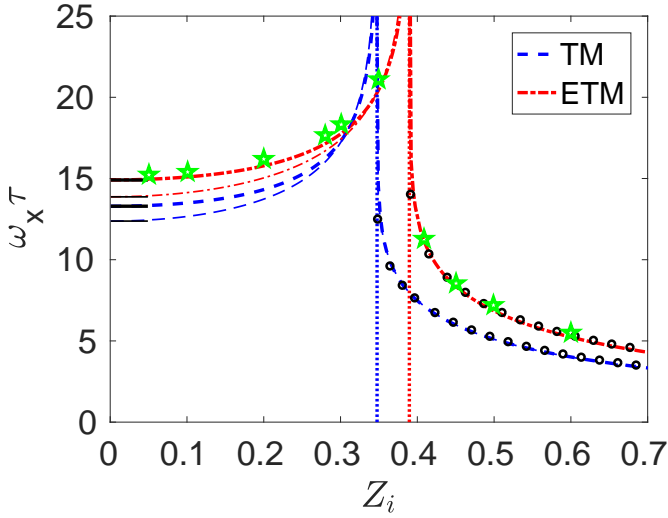


Fig. 4. (color online) Trajectory periods as functions of the initial imbalance Z_i for the TM (dashed blue lines) and ETM (dash-dotted red lines) models according to Eq. (15) with $\varphi_i = 0$. Thinner lines correspond to calculations neglecting γ . The vertical lines mark the critical imbalance Z_c , while the circles correspond to Eq. (26) for the TM and ETM models and the horizontal solid lines correspond to the small-oscillation approximations. The stars indicate the periods obtained from the full 3D GP simulation.

We also compare in Fig. 5 the exact results for $\gamma = 0$ in the ST regime with the value of τ_0 given by Eq. (19), and with T_{st} , Eq. (26). In particular, we show the results for $\Lambda = 16, 25.5$, and 64 , where it may be seen that our estimate, T_{st} , provides a simple and improved overall approximation around an extended region in Z_i . For lower values of Λ the assumption $\Lambda \gg 1$ breaks down and hence both approximations become less accurate. For larger values both estimates get closer to the exact result, while our prediction is able to quantitatively describe the exact curve closer to Z_c much better than τ_0 . For values above $\Lambda \simeq 10^3$ despite the error is substantially reduced in both approximations, T_{st} still improves the period calculation over τ_0 .

5 Summary and concluding remarks

We have studied the dynamics of three-dimensional Bose-Einstein condensates using a two-mode model with an effective on-site interaction parameter and compare it to the full 3D Gross-Pitaevskii simulations. We demonstrate that the periods of the orbits for two-mode models with arbitrary initial conditions can be written as a closed integral form which takes into account the effect of the overlap between the localized densities through the parameter γ . We show that this interaction-driven effect is specially important in the Josephson regime for the experimental conditions of [5]. Furthermore, based on the dynamical equations for the populations and phase differences in each well, we have derived a simple analytical formula for the period in the self-trapping regime, which accurately re-

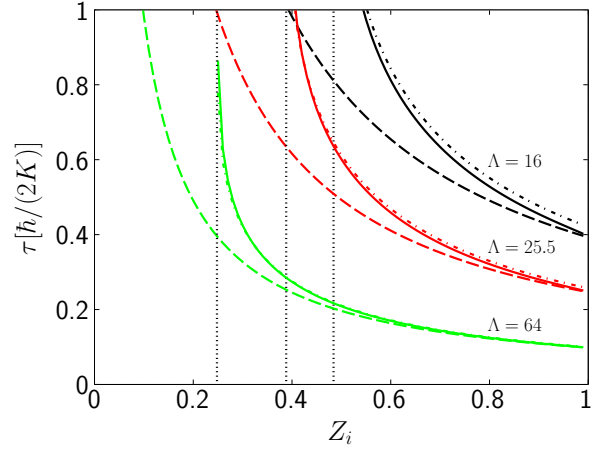


Fig. 5. (color online) Comparison of the time periods τ (in units of $\hbar/(2K)$) in different approximations for $\Lambda = 16, 25.5$, and 64 . The solid, dashed, and dash-dotted lines correspond to the exact results (15), the approximation τ_0 (19), and T_{st} given by Eq. (26), respectively. The vertical dotted lines mark the critical imbalance Z_c for each value of Λ .

produces the exact integral expression of the two-mode model and correctly describes Gross-Pitaevskii simulation results for large on-site interaction energy parameters.

The three-dimensional numerical simulations prove that the precise determination of the effective on-site interaction energy parameter is essential to correctly reproduce the GP results and thus to calculate accurate estimates of the time periods.

The present study opens the possibility to the application of the effective two-mode model and the time period expressions to multiple-well systems with symmetric initial populations. In such cases, the dynamics can be characterized by a single imbalance and a phase difference in terms of which the two-mode Hamiltonian can be easily furnished. Studies in such direction are currently underway for a four-well system.

This work was supported by CONICET and Universidad de Buenos Aires through grants PIP 11220150100442CO and UBA-CyT 20020150100157, respectively.

Author contribution statement

All authors contributed equally to the paper.

Appendix A. Multimode Parameters

The parameters of the TM model are defined as

$$J = - \int d^3\mathbf{r} \, \psi_R(\mathbf{r}) \left[-\frac{\hbar^2}{2m} \nabla^2 + V_{\text{trap}}(\mathbf{r}) \right] \psi_L(\mathbf{r}) \quad (\text{A.1})$$

$$U = g \int d^3\mathbf{r} \, \psi_R^4(\mathbf{r}) \quad (\text{A.2})$$

$$F = -gN \int d^3\mathbf{r} \psi_R^3(\mathbf{r})\psi_L(\mathbf{r}) \quad (\text{A.3})$$

$$I = gN \int d^3\mathbf{r} \psi_R^2(\mathbf{r})\psi_L^2(\mathbf{r}). \quad (\text{A.4})$$

where $\psi_R(\mathbf{r})$ and $\psi_L(\mathbf{r})$ are the localized modes at the right and left sides, respectively. As usual the left (right) mode is obtained from the sum (difference) of the lowest energy symmetric and antisymmetric stationary order parameters obtained from the GP equation. The interaction-driven parameters F and I were first defined in [3] and later analyzed in [4].

Together with the calculation of these parameters through the preceding definitions, we have applied also the alternative method outlined in [23], finding an agreement between both procedures with a precision higher than 99%. In particular, we note that the difference of energies between antisymmetric and ground states of the TM model defines the hopping parameter K [31].

References

1. A. Smerzi, S. Fantoni, S. Giovanazzi and S. R. Shenoy, Phys. Rev. Lett. **79**, 4950 (1997).
2. S. Raghavan, A. Smerzi, S. Fantoni and S. R. Shenoy, Phys. Rev. A **59**, 620 (1999).
3. D. Ananikian and T. Bergeman, Phys. Rev. A **73**, 013604 (2006).
4. X. Jia, W. Li and J. Q. Liang, Phys. Rev. A **78**, 023613 (2008).
5. M. Albiez, R. Gati, J. Fölling, S. Hunsmann, M. Cristiani and M. K. Oberthaler, Phys. Rev. Lett. **95**, 010402 (2005).
6. M. Melé-Messeguer, B. Juliá-Díaz, M. Guilleumas, A. Polls and A. Sanpera, New J. Phys. **13**, 033012 (2011).
7. M. Abad, M. Guilleumas, R. Mayol, M. Pi and D. M. Jezek, Europhys. Lett. **94**, 10004 (2011).
8. T. Mayteevarunyoo, B. A. Malomed and G. Dong, Phys. Rev. A **78**, 053601 (2008).
9. B. Xiong, J. Gong, H. Pu, W. Bao and B. Li, Phys. Rev. A **79**, 013626 (2009).
10. Q. Zhou, J. V. Porto and S. Das Sarma, Phys. Rev. A **84**, 031607 (2011).
11. B. Cui, L. C. Wang and X. X. Yi, Phys. Rev. A **82**, 062105 (2010).
12. M. Abad, M. Guilleumas, R. Mayol, M. Pi and D. M. Jezek, Phys. Rev. A **84**, 035601 (2011).
13. C. E. Creffield, Phys. Rev. A **75**, 031607(R) (2007).
14. J.-K. Xue, A.-X. Zhang and J. Liu, Phys. Rev. A **77**, 013602 (2008).
15. T. J. Alexander, E. A. Ostrovskaya and Y. S. Kivshar, Phys. Rev. Lett. **86**, 040401 (2006).
16. B. Liu, L.-B. Fu, S.-P. Yang and J. Liu, Phys. Rev. A **75**, 033601 (2007).
17. Th. Anker, M. Albiez, R. Gati, S. Hunsmann, B. Eiermann, A. Trombettoni and M. K. Oberthaler, Phys. Rev. Lett. **94**, 020403 (2005).
18. B. Wang, P. Fu, J. Liu and B. Wu, Phys. Rev. A **74**, 063610 (2006).
19. A. R. Kolovsky, Phys. Rev. A **82**, 011601(R) (2010); S. K. Adhikari, J. Phys. B.: At. Mol. Opt. Phys. **44**, 075301 (2011).
20. K. Henderson, C. Ryu, C. MacCormick and M. G. Boshier, New J. Phys. **11**, 043030 (2009).
21. T. F. Viscondi and K. Furuya, J. Phys. A **44**, 175301 (2011).
22. S. De Liberato and C. J. Foot, Phys. Rev. A **73**, 035602 (2006).
23. D. M. Jezek and H. M. Cataldo, Phys. Rev. A **88**, 013636 (2013).
24. D. M. Jezek, P. Capuzzi and H. M. Cataldo, Phys. Rev. A **87**, 053625 (2013).
25. M. Albiez, Ph.D. thesis, University of Heidelberg, 2005.
26. M. Abad, M. Guilleumas, R. Mayol, F. Piazza, D. M. Jezek and A. Smerzi, Europhys. Lett. **109**, 40005 (2015).
27. Y. Huang, Q.-S. Tan, L.-B. Fu and X. Wang, Phys. Rev. A **88**, 063642 (2013).
28. L. Fu and J. Liu Phys. Rev. A, **74** 063614 (2006).
29. W. H. Press, S. A. Teukolsky, W. T. Vetterling, and B. P. Flannery, Numerical Recipes: The Art of Scientific Computing, 3rd ed. (Cambridge University Press, New York, 2007).
30. Weizhu Bao, Dieter Jaksch, and Peter A. Markowich, J. Comput. Phys. **187**, 318 (2003).
31. L. J. LeBlanc, A. B. Bardson, J. McKeever, M. H. T. Extavour, D. Jervis, J. H. Thywissen, F. Piazza and A. Smerzi, Phys. Rev. Lett. **106**, 025302 (2011).